1000+ FPS 4D Gaussian Splatting for Dynamic Scene Rendering

Yuheng Yuan[1,*] **Qiuhong Shen**[1,*] **Xingyi Yang**[2,1] **Xinchao Wang**[1,†]
[1]National University of Singapore [2]The Hong Kong Polytechnic University
{yuhengyuan,qiuhong.shen}@u.nus.edu, xingyi.yang@polyu.edu.hk, xinchao@nus.edu.sg
Project page: https://4dgs-1k.github.io/

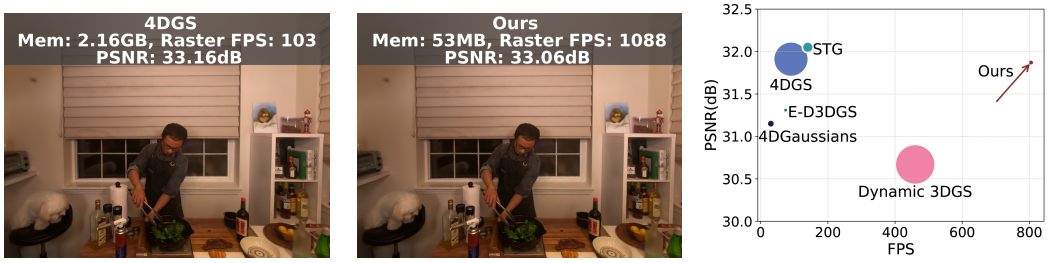

Figure 1: **Compressibility and Rendering Speed.** We introduce **4DGS-1K**, a novel compact representation with high rendering speed. In contrast to 4D Gaussian Splatting (4DGS) [1], we can achieve rasterization at 1000+ FPS while maintaining comparable photorealistic quality with only 2% of the original storage size. The right figure is the result tested on the N3V [2] datasets, where the radius of the dot corresponds to the storage size.

Abstract

4D Gaussian Splatting (4DGS) has recently gained considerable attention as a method for reconstructing dynamic scenes. Despite achieving superior quality, 4DGS typically requires substantial storage and suffers from slow rendering speed. In this work, we delve into these issues and identify two key sources of temporal redundancy. (Q1) **Short-Lifespan Gaussians**: 4DGS uses a large portion of Gaussians with short temporal span to represent scene dynamics, leading to an excessive number of Gaussians. (Q2) **Inactive Gaussians**: When rendering, only a small subset of Gaussians contributes to each frame. Despite this, all Gaussians are processed during rasterization, resulting in redundant computation overhead. To address these redundancies, we present **4DGS-1K**, which runs at over 1000 FPS on modern GPUs. For Q1, we introduce the Spatial-Temporal Variation Score, a new pruning criterion that effectively removes short-lifespan Gaussians while encouraging 4DGS to capture scene dynamics using Gaussians with longer temporal spans. For Q2, we store a mask for active Gaussians across consecutive frames, significantly reducing redundant computations. Compared to vanilla 4DGS, our method achieves a $41\times$ reduction in storage and $9\times$ faster rasterization on complex dynamic scenes, while maintaining comparable visual quality.

1 Introduction

Novel view synthesis for dynamic scenes allows for the creation of realistic representations of 4D environments, which is essential in fields like computer vision, virtual reality, and augmented reality. Traditionally, this area has been led by neural radiance fields (NeRF) [2–6], which model opacity and

[*]Equal contribution.
[†]Corresponding Author.

39th Conference on Neural Information Processing Systems (NeurIPS 2025).

color over time to depict dynamic scenes. While effective, these NeRF-based methods come with high training and rendering costs, limiting their practicality, especially in real-time applications and on devices with limited resources.

Recently, point-based representations like 4D Gaussian Splatting (4DGS) [1] have emerged as strong alternatives. 4DGS models a dynamic scene using a set of 4D Gaussian primitives, each with a 4-dimensional mean and a 4×4 covariance matrix. At any given timestamp, a 4D Gaussian is decomposed into a set of conditional 3D Gaussians and a marginal 1D Gaussian, the latter controlling the opacity at that moment. This mechanism allows 4DGS to effectively capture both static and dynamic features of a scene, enabling high-fidelity dynamic scene reconstruction.

However, representing dynamic scenes with 4DGS is both storage-intensive and slow. Specifically, 4DGS often requires millions of Gaussians, leading to significant storage demands (averaging 2GB for each scene on the N3V [2] dataset) and suboptimal rendering speed. In comparison, mainstream deformation field methods [7] require only about 90MB for the same dataset. Therefore, reducing the storage size of 4DGS [1] and improving rendering speed are essential for efficiently representing complex dynamic scenes.

We look into the cause of such an explosive number of Gaussian and place a specific emphasis on two key issues. **(Q1)** A large portion of Gaussians exhibit a short temporal span. In empirical experiments, 4DGS tends to favor "flicking" Gaussians to fit complex dynamic scenes, which just influence a short portion of the temporal domain. This necessitates that 4DGS relies on a large number of Gaussians to reconstruct a high-fidelity scene. As a result, substantial storage is needed to record the attributes of these Gaussians. **(Q2)** Inactive Gaussians lead to redundant computation. During rendering, 4DGS needs to process all Gaussians. However, only a very small portion of Gaussians are active at that moment. Therefore, most of the computation time is spent on inactive Gaussians. This phenomenon greatly hampers the rendering speed. In this paper, we introduce **4DGS-1K**, a framework that significantly reduces the number of Gaussians to minimize storage requirements and speedup rendering while maintaining high-quality reconstruction. To address these issues, 4DGS-1K introduces a two-step pruning approach:

- **Pruning Short-Lifespan Gaussians.** We propose a novel pruning criterion called the *spatial-temporal variation score*, which evaluates the temporal impact of each Gaussian. Gaussians with minimal influence are identified and pruned, resulting in a more compact scene representation with fewer Gaussians with short temporal span.
- **Filtering Inactive Gaussians.** To further reduce redundant computations during rendering, we use a key-frame temporal filter that selects the Gaussians needed for each frame. On top of this, we share the masks for adjacent frames. This is based on our observation that Gaussians active in adjacent frames often overlap significantly.

Besides, the pruning in step 1 enhances the masking process in step 2. By pruning Gaussians, we increase the temporal influence of each Gaussian, which allows us to select sparser key frames and further reduce storage requirements.

We have extensively tested our proposed model on various dynamic scene datasets including real and synthetic scenes. As shown in Figure 1, 4DGS-1K reduces storage costs by $41\times$ on the Neural 3D Video datasets [2] while maintaining equivalent scene representation quality. Crucially, it enables real-time rasterization speeds exceeding 1,000 FPS. These advancements collectively position 4DGS-1K as a practical solution for high-fidelity dynamic scene modeling without compromising efficiency.

In summary, our contributions are three-fold:

- We delve into the temporal redundancy of 4D Gaussian Splatting, and explain the main reason for the storage pressure and suboptimal rendering speed.
- We introduce **4DGS-1K**, a compact and memory-efficient framework to address these issues. It consists of two key components, a spatial-temporal variation score-based pruning strategy and a temporal filter.
- Extensive experiments demonstrate that 4DGS-1K not only achieves a substantial storage reduction of approximately $41\times$ but also accelerates rasterization to 1000+ FPS while maintaining high-quality reconstruction.

2 Related Work

2.1 Novel view synthesis for static scenes

Recently, neural radiance fields(NeRF) [3] have achieved encouraging results in novel view synthesis. NeRF [3] represents the scene by mapping 3D coordinates and view dependency to color and opacity. Since NeRF [3] requires sampling each ray by querying the MLP for hundreds of points, this significantly limits the training and rendering speed. Subsequent studies [8–15] have attempted to speed up the rendering by introducing specialized designs. However, these designs also constrain the widespread application of these models. In contrast, 3D Gaussian Splatting(3DGS) [16] has gained significant attention, which utilizes anisotropic 3D Gaussians to represent scenes. It achieves high-quality results with intricate details, while maintaining real-time rendering performance.

2.2 Novel view synthesis for dynamic scenes

Dynamic NVS poses new challenges due to the temporal variations in the input images. Previous NeRF-based dynamic scene representation methods [2, 4–6, 17–22] handle dynamic scenes by learning a mapping from spatiotemporal coordinates to color and density. Unfortunately, these NeRF-based models are constrained in their applications due to low rendering speeds. Recently, 3D Gaussians Splatting [16] has emerged as a novel explicit representation, with many studies [7, 23–27] attempting to model the dynamic scenes based on it. 4D Gaussian Splatting(4DGS) [1] is one of the representatives. It utilizes a set of 4D Gaussian primitives. However, 4DGS often requires a huge redundant number of Gaussians for dynamic scenes. These Gaussians lead to tremendous storage and suboptimal rendering speed. To this end, we focus on analyzing the temporal redundancy of 4DGS [1] in hopes of developing a novel framework to achieve lower storage requirements and higher rendering speeds.

2.3 Gaussian Splatting Compression

3D Gaussian-based large-scale scene reconstruction typically requires millions of Gaussians, resulting in the requirement of up to several gigabytes of storage. Therefore, subsequent studies have attempted to tackle these issues. Specifically, Compgs [28] and Compact3D [29] employ vector quantization to store Gaussians within codebooks. Concurrently, inspired by model pruning, some studies [30–35] have proposed criterion to prune Gaussians by a specified ratio. However, compared to 3DGS [16], 4DGS [1] introduces an extra temporal dimension to enable dynamic representation. Previous 3DGS-based methods may therefore be unsuitable for 4DGS. Consequently, we first identify a key limitation leading to this problem, referred as *temporal redundancy*. Furthermore, we propose a novel pruning criterion leveraging spatial-temporal variation, and a temporal filter to achieve more efficient storage requirements and higher rendering speed.

3 Preliminary of 4D Gaussian Splatting

Our framework builds on 4D Gaussian Splatting (4DGS) [1], which reconstructs dynamic scenes by optimizing a collection of *anisotropic 4D Gaussian primitives*. For each Gaussian, it is characterized by a 4D mean $\mu = (\mu_x, \mu_y, \mu_z, \mu_t) \in \mathbb{R}^4$ coupled with a covariance matrix $\Sigma \in \mathbb{R}^{4\times4}$.

By treating time and space dimensions equally, the 4D covariance matrix Σ can be decomposed into a scaling matrix $S_{4D} = (s_x, s_y, s_z, s_t) \in \mathbb{R}^4$ and a rotation matrix $R_{4D} \in \mathbb{R}^{4\times4}$. R_{4D} is represented by a pair of left quaternion $q_l \in \mathbb{R}^4$ and right quaternion $q_r \in \mathbb{R}^4$.

During rendering, each 4D Gaussian is decomposed into a conditional 3D Gaussian and a 1D Gaussian at a specific time t. Moreover, the conditional 3D Gaussian can be derived from the properties of the multivariate Gaussian with:

$$\begin{aligned} \mu_{xyz|t} &= \mu_{1:3} + \Sigma_{1:3,4}\Sigma_{4,4}^{-1}(t - \mu_t) \\ \Sigma_{xyz|t} &= \Sigma_{1:3,1:3} - \Sigma_{1:3,4}\Sigma_{4,4}^{-1}\Sigma_{4,1:3} \end{aligned} \tag{1}$$

Here, $\mu_{1:3} \in \mathbb{R}^3$ and $\Sigma_{1:3,1:3} \in \mathbb{R}^{3\times3}$ denote the spatial mean and covariance, while μ_t and $\Sigma_{4,4}$ are scalars representing the temporal components. To perform rasterization, given a pixel under view $\mathcal{I}$

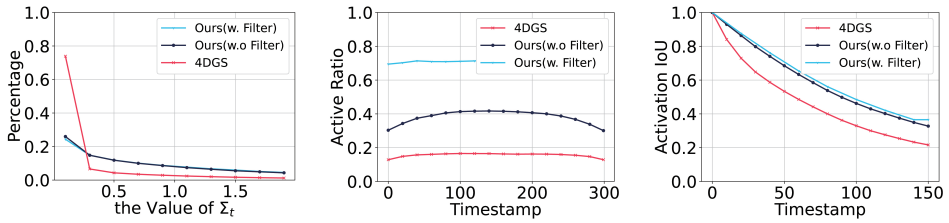

(a) (b) (c)

Figure 2: **Temporal redundancy Study.** (a) The Σ_t distribution of 4DGS. The red line shows the result of vanilla 4DGS. The other two lines represent our model has effectively reduced the number of transient Gaussians with small Σ_t. (b) The active ratio during rendering at different timestamps. It demonstrates that most of the computation time is spent on inactive Gaussians in vanilla 4DGS. However, 4DGS-1K can significantly reduce the occurrence of inactive Gaussians during rendering to avoid unnecessary computations. (c) This figure shows the IoU between the set of active Gaussians in the first frame and frame t. It proves that active Gaussians tend to overlap significantly across adjacent frames.

and timestamp t, its color $\mathcal{I}(u, v, t)$ can be computed by blending visible Gaussians that are sorted by their depth:

$$\mathcal{I}(u, v, t) = \sum_{i}^{N} c_i(d)\alpha_i \prod_{j=1}^{i-1}(1 - \alpha_j) \tag{2}$$

with

$$\begin{aligned} \alpha_i &= p_i(t)p_t(u, v|t)\sigma_i \\ p_i(t) &\sim \mathcal{N}(t; \mu_t, \Sigma_{4,4}) \end{aligned} \tag{3}$$

where $c_i(d)$ is the color of each Gaussian, and α_i is given by evaluating a 2D Gaussian with covariance Σ_{2D} multiplied with a learned per-point opacity σ_i and temporal Gaussian distribution $p_i(t)$. In the following discussion, we denote $\Sigma_{4,4}$ as Σ_t for simplicity.

Temporal Redundancy. Despite achieving high quality, 4DGS requires a huge number of Gaussians to model dynamic scenes. We identify a key limitation leading to this problem: 4DGS represents scenes through temporally independent Gaussians that lack explicit correlation across time. This means that, even static objects are redundantly represented by hundreds of Gaussians, which inconsistently appear or vanish across timesteps. We refer to this phenomenon as *temporal redundancy*. As a result, scenes end up needing more Gaussians than they should, leading to excessive storage demands and suboptimal rendering speeds. In Section 4, we analyze the root causes of this issue and propose a set of solutions to reduce the count of Gaussians.

4 Methodology

Our goal is to compress 4DGS by reducing the number of Gaussians while preserving rendering quality. To achieve this, we first analyze the redundancies present in 4DGS, as detailed in Section 4.1. Building on this analysis, we introduce 4DGS-1K in Section 4.2, which incorporates a set of compression techniques designed for 4DGS. 4DGS-1K enables rendering speeds of over 1,000 FPS on modern GPUs.

4.1 Understanding Redundancy in 4DGS

This section investigates why 4DGS requires an excessive number of Gaussians to represent dynamic scenes. In particular, we identify two key factors. First, 4DGS models object motion using a large number of transient Gaussians that inconsistently appear and disappear across timesteps, leading to redundant temporal representations. Second, for each frame, only a small fraction of Gaussians actually contribute to the rendering. We discuss those problems below.

Massive Short-Lifespan Gaussians. We observe that 4DGS tends to store numerous Gaussians that flicker in time. We refer to these as *Short-Lifespan Gaussians*. To investigate this property,

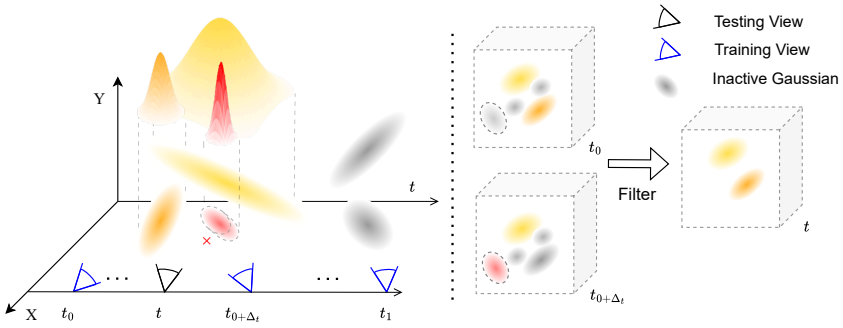

(a) Transient Gaussian Pruning (b) Temporal Filter

Figure 3: **Overview of 4DGS-1K.** (a) We first calculate the spatial-temporal variation score for each 4D Gaussian on training views, to prune Gaussians with short lifespan (The Red Gaussian). (b) The temporal filter is introduced to filter out inactive Gaussians before the rendering process to alleviate suboptimal rendering speed. At a given timestamp t, the set of Gaussians participating in rendering is derived from the two adjacent key-frames, t_0 and $t_{0+\Delta_t}$.

we analyze the Gaussians' opacity, which controls visibility. Intuitively, Short-Lifespan Gaussians exhibit an opacity pattern that rapidly increases and then suddenly decreases. In 4DGS, this behavior is typically reflected in the time variance parameter Σ_t—small Σ_t values indicate a short lifespan.

Observations. Specifically, we plot the distribution of Σ_t for all Gaussians in the *Sear Steak* scene. As shown in Figure 2a, most of Gaussians has small Σ_t values (e.g. 70% have $\Sigma_t < 0.25$).

Therefore, in 4DGS, nearly all Gaussians have a short lifespan. This property leads to high storage needs and slower rendering.

Inactive Gaussians. Another finding is that, during the forward rendering, actually, only a small fraction of Gaussians are contributing. Interestingly, active ones tend to overlap significantly across adjacent frames. To quantify this, we introduce two metrics: (1) *Active ratio*. This ratio is defined as the proportion of the total number of active Gaussians across all views at any moment relative to the total number of Gaussians. (2) *Activation Intersection-over-Union (IoU)*. This is computed as IoU between the set of active Gaussians in the first frame and in frame t.

Observations. Again, we plot the two metrics from *Sear Steak* scene. As shown in Figure 2b, nearly 85% of Gaussians are inactive at each frame, even though all Gaussians are processed during rendering. Moreover, Figure 2c demonstrates that the active Gaussians remain quite consistent over time, with an IoU above 80% over a 20-frame window.

The inactive gaussians bring a significant issue in 4DGS, because each 4D Gaussian must be decomposed into a 3D Gaussian and a 1D Gaussian before rasterization (see eq. (1)). Therefore, a large portion of computational resources is wasted on inactive Gaussians.

In summary, redundancy in 4DGS comes from massive Short-Lifespan Gaussians and inactive Gaussians. These insights motivate our compression strategy to eliminate redundant computations while preserving rendering quality.

4.2 4DGS-1K for Fast Dynamic Scene Rendering

Building on the analysis above, we introduce 4DGS-1K, a suite of compression techniques specifically designed for 4DGS to eliminate redundant Gaussians. As shown in Figure 3, this process involves two key steps. First, we identify and globally prune unimportant Gaussians with low Spatial-Temporal Variation Score in Section 4.2.1. Second, we apply local pruning using a temporal filter to inactive Gaussians that are not needed at each timestep in Section 4.2.2.

4.2.1 Pruning with Spatial-Temporal Variation Score

We first prune unimportant 4D Gaussians to improve efficiency. Like 3DGS, we remove those that have a low impact on rendered pixels. Besides, we additionally remove short-lifespan Gaus-

sians—those that persist only briefly over time. To achieve this, we introduce a novel spatial-temporal variation score as the pruning criterion for 4DGS. It is composed of two parts, *spatial score* that measures the Gaussians contributions to the pixels in rendering, and *temporal score* considering the lifespan of Gaussians.

Spatial score. Inspired by the previous method [30, 31] and α-blending in 3DGS [16], we define the spatial score by aggregating the ray contribution of Gaussian g_i along all rays r across all input images at a given timestamp. It can accurately capture the contribution of each Gaussian to one pixel. Consequently, the spatial contribution score $\mathcal{S}^S$ is obtained by traversing all pixels:

$$\mathcal{S}_i^S = \sum_{k=1}^{NHW} \alpha_i \prod_{j=1}^{i-1}(1-\alpha_j) \tag{4}$$

where N denotes the number of training views, H, W denote the height and width of the images, and $\alpha_i \prod_{j=1}^{i-1}(1-\alpha_j)$ reflects the contribution of i^{th} Gaussian to the final color of all pixels according to the alpha composition in eq. (2).

Temporal score. It is expected to assign a higher temporal score to Gaussians with a longer lifespan. To quantify this, we compute the *second derivative of* temporal opacity function $p_i(t)$ defined in eq. (3). The second derivative $p_i^{(2)}(t)$ is computed as

$$p_i^{(2)}(t) = (\frac{(t-\mu_t)^2}{\Sigma_t^2} - \frac{1}{\Sigma_t})p_i(t) \tag{5}$$

Intuitively, large second derivative magnitude corresponds to unstable, short-lived Gaussians, while low second derivative indicates smooth, persistent ones.

Moreover, since the second derivative spans the real number domain $\mathbb{R}$, we apply $\tanh$ function to map it to the interval $(0, 1)$. Consequently, the score for opacity variation, $\mathcal{S}_i^{TV}$, of each Gaussian $g_{i,t}$ is expressed as:

$$\mathcal{S}_i^{TV} = \sum_{t=0}^{T} \frac{1}{0.5 \cdot \tanh(\left|p_i^{(2)}(t)\right|) + 0.5}. \tag{6}$$

In addition to the opacity range rate, the volume of 4D Gaussians is necessary to be considered, as described in eq. (1). The volume should be normalized following the method in [30], denoted as $\gamma(\mathcal{S}^{4D}) = Norm(V(\mathcal{S}^{4D}))$. Therefore, the final temporal score $\mathcal{S}_i^T = \mathcal{S}_i^{TV}\gamma(S_i^{4D})$

Finally, by aggregating both spatial and temporal score, the spatial-temporal variation score $\mathcal{S}_i$ can be written as:

$$\mathcal{S}_i = \sum_{t=0}^{T} \mathcal{S}_i^T \mathcal{S}_i^S \tag{7}$$

Pruning. All 4D Gaussians are ranked based on their spatial-temporal variation score $\mathcal{S}_i$, and Gaussians with lower scores are pruned to reduce the storage burden of 4DGS [1]. The remaining Gaussians are optimized over a set number of iterations to compensate for minor losses resulting from pruning.

4.2.2 Fast rendering with temporal filtering

Our analysis reveals that inactive Gaussians induces unnecessary computations in 4DGS, significantly slowing down rendering. To address this issue, we introduce a temporal filter that dynamically selects active Gaussians. We observed that active Gaussians in adjacent frames overlap considerably (as detailed in Section 4.1), which allows us to share their corresponding masks across a window of frames.

Key-frame based Temporal Filtering. Based on this observation, we design a key-frame based temporal filtering for active Gaussians. We select sparse key-frames at even intervals and share their masks with surrounding frames.

Specifically, we select a list of key-frame timestamps $\{t_i\}_{i=0}^{T}$, where T depends on the chosen interval Δ_t. For each t_i, we render the images from all training views at current timestamp and calculate the visibility list $\{m_{i,j}\}_{j=1}^{N}$, where $m_{i,j}$ is the visibility mask obtained by eq. (2) from the j^{th} training

Table 1: **Quantitative comparisons on the Neural 3D Video Dataset.**

Method	PSNR↑	SSIM↑	LPIPS↓	Storage(MB)↓	FPS↑	Raster FPS↑	#Gauss↓
Neural Volume[1][4]	22.80	-	0.295	-	-	-	-
DyNeRF[1][2]	29.58	-	0.083	28	0.015	-	-
StreamRF[18]	28.26	-	-	5310	10.90	-	-
HyperReel[5]	31.10	0.927	0.096	360	2.00	-	-
K-Planes[6]	31.63	-	0.018	311	0.30	-	-
4K4D[36]	21.29	-	-	2519	290	-	-
Dynamic 3DGS[37]	30.67	0.930	0.099	2764	460	-	-
4DGaussian[7]	31.15	0.940	0.049	90	30	-	-
E-D3DGS[26]	31.31	0.945	0.037	35	74	-	-
Swift4D[38]	32.23	-	0.043	120	125	-	-
Grid4D[39]	31.49	-	-	146	116	-	-
STG[40]	32.05	0.946	0.044	200	140	-	-
4D-RotorGS[41]	31.62	0.940	0.140	-	277	-	-
MEGA[42]	31.49	-	0.056	25	77	-	-
Compact3D[29]	31.69	0.945	0.054	15	186	-	-
4DGS[1]	32.01	-	0.055	-	114	-	-
4DGS[2][1]	31.91	0.946	0.052	2085	90	118	3333160
Ours	31.88	0.946	0.052	418	**805**	**1092**	666632
Ours-PP	31.87	0.944	0.053	**50**	805	1092	666632

[1] The metrics of the model are tested without "coffee martini" and the resolution is set to 1024×768.

[2] The retrained model from the official implementation.

Table 2: **Quantitative comparisons on the D-NeRF Dataset.**

Method	PSNR↑	SSIM↑	LPIPS↓	Storage(MB)↓	FPS↑	Raster FPS↑	#Gauss↓
DNeRF[19]	29.67	0.95	0.08	-	0.1	-	-
TiNeuVox[43]	32.67	0.97	0.04	-	1.6	-	-
K-Planes[6]	31.07	0.97	0.02	-	1.2	-	-
4DGaussian[7]	32.99	0.97	0.05	18	104	-	-
Deformable3DGS[23]	40.43	0.99	0.01	27	70	-	131428
SC-GS[44]	40.65	-	-	28	126	-	-
Grid4D[39]	39.91	-	-	93	166	-	-
4D-RotorGS[41]	34.26	0.97	0.03	112	1257	-	-
4DGS[1]	34.09	0.98	0.02	-	-	-	-
4DGS[1][1]	32.99	0.97	0.03	278	376	1232	445076
Ours	33.34	0.97	0.03	42	**1462**	**2482**	66460
Ours-PP	33.37	0.97	0.03	**7**	1462	2482	66460

[1] The retrained model from the official implementation.

viewpoint at timestamp t_i and N is the number of training views at current timestamp. The final set of active Gaussian masks is given by $\left\{\bigcup_{j=1}^{N} m_{i,j}\right\}_{i=0}^{T}$.

Filter based Rendering. To render the images from any viewpoint at a given timestamp t_{test}, we consider its two nearest key-frames, denoted as t_l and t_r. Then, we perform rasterization while only considering the Gaussians marked by mask $\left\{\bigcup_{j=1}^{N} m_{i,j}\right\}_{i=l,r}$. This method explicitly filters out inactive Gaussians to speed up rendering.

Note that using long intervals may overlook some Gaussians, reducing rendering quality. Therefore, we fine-tune Gaussians recorded by the masks to compensate for losses.

5 Experiment

5.1 Experimental Settings

Datasets. We utilize two dynamic scene datasets to demonstrate the effectiveness of our method: (1) **Neural 3D Video Dataset (N3V)** [2]. This dataset consists of six dynamic scenes, and the resolution is 2704×2028. For a fair comparison, we align with previous work [1, 40] by conducting evaluations at a half-resolution of 300 frames. (2) **D-NeRF Dataset** [19]. This dataset is a monocular video dataset comprising eight videos of synthetic scenes. We choose standard test views that originate from novel camera positions not encountered during the training process.

Evaluation Metrics. To evaluate the quality of rendering dynamic scenes, we employ several commonly used image quality assessment metrics: Peak Signal-to-Noise Ratio (PSNR), Structural

(a) Results on Sear Steak Scene.

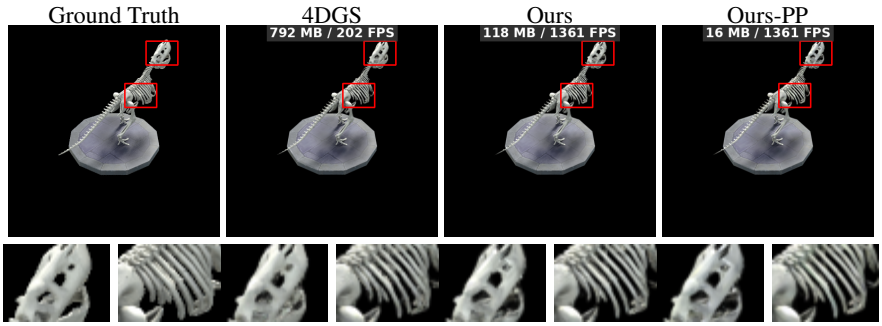

(b) Results on Trex Scene.

Figure 4: **Qualitative comparisons of 4DGS and our method.**

Table 3: **Ablation study of per-component contribution.**

ID	Method\Dataset			PSNR↑	SSIM↑	LPIPS↓	Storage(MB)↓	FPS↑	Raster FPS↑	#Gauss↓
	Filter	Pruning	PP							
a	vanilla 4DGS[1]			31.91	0.9458	0.0518	2085	90	118	3333160
b	✓[1,2]			31.51	0.9446	0.0539	2091	242	561	3333160
c	✓[2]			29.56	0.9354	0.0605	2091	300	561	3333160
d		✓		31.92	0.9462	0.0513	417	312	600	666632
e	✓	✓		31.88	0.9457	0.0524	418	805	1092	666632
f	✓[2]	✓		31.63	0.9452	0.0524	418	789	1080	666632
g	✓	✓	✓	31.87	0.9444	0.0532	50	805	1092	666632

[1] The result with environment map. [2] The result without finetuning.

Similarity Index Measure (SSIM), and Learned Perceptual Image Patch Similarity (LPIPS) [45]. Following the previous work, LPIPS [45] is computed using AlexNet [46] and VGGNet [47] on the N3V dataset and the D-NeRF dataset, respectively. Moreover, we report the number of Gaussians and storage. To demonstrate the improvement in rendering speed, we report two types of FPS: (1) **FPS.** It considers the entire rendering function. Due to interference from other operations, it can't effectively demonstrate the acceleration achieved by our method. (2) **Raster FPS.** It only considers the rasterization, the most computationally intensive component during rendering.

Baselines. Our primary baseline for comparison is 4DGS [1], which serves as the foundation of our model. Moreover, we compare 4DGS-1K with two concurrent works on 4D compression, MEGA [42] and Compact3D [29]. Certainly, we conduct comparisons with 4D-RotorGS [41] which is another form of representation for 4D Gaussian Splatting with the capability for real-time rendering speed and high-fidelity rendering results. In addition, we also compare our work against NeRF-based methods, like Neural Volume [4], DyNeRF [2], StreamRF [18], HyperReel [5], DNeRF [19], K-Planes [6] and 4K4D [36]. Furthermore, other recent competitive Gaussian-based methods are also considered in our comparison, including Dynamic 3DGS [37], STG [40], 4DGaussian [7], E-D3DGS [26], Swift4D [38], Grid4D [39] and SC-GS [44].

Implementation Details. Our method is tested in a single RTX 3090 GPU. We train our model following the experiment setting in 4DGS [1]. After training, we perform the pruning and filtering strategy. Then, we fine-tune 4DGS-1K for 5,000 iterations while disabling additional clone/split operations. For pruning strategy, the pruning ratio is set to 80% on the N3V Dataset, and 85% on the D-NeRF Dataset. For the temporal filtering, we set the interval Δ_t between key-frames to 20 frames

on the N3V Dataset. Considering the varying capture speeds on the D-NeRF dataset, we select 6 key-frames rather than a specific frame interval. Additionally, to further compress the storage of 4DGS [1], we implement post-processing techniques in our model, denoted as Ours-PP. It includes vector quantization [28] on SH of Gaussians and compressing the mask of filter into bits.

Note that we don't apply environment maps implemented by 4DGS on Coffee Martini and Flame Salmon scenes, which significantly affects the rendering speed. Subsequent results indicate that removing it for 4DGS-1K does not significantly degrade the rendering quality.

5.2 Results and Comparisons

Comparisons on real-world dataset. Table 1 presents a quantitative evaluation on the N3V dataset. 4DGS-1K achieves rendering quality comparable to the current baseline. Compared to 4DGS [1], we achieve a $41\times$ compression and $9\times$ faster in rendering speed at the cost of a $0.04dB$ reduction in PSNR. In addition, compared to MEGA [42] and Compact3D [29], two concurrent works on 4D compression, the rendering speeds are $10\times$ and $4\times$ faster respectively while maintaining a comparable storage requirement and high quality reconstruction. Moreover, the FPS of 4DGS-1K far exceeds the current state-of-the-art levels. It is nearly twice as fast as the current fastest model, Dynamic 3DGS [37] while requiring only **1%** of the storage size. Additionally, 4DGS-1K achieves better visual quality than that of Dynamic 3DGS [37], with an increase of about $1.2dB$ in PSNR. Compared to the storage-efficient model, E-D3DGS [26] and DyNeRF [2] we achieve an increase of over $0.5dB$ in PSNR and fast rendering speed. Figure 4 offers qualitative comparisons for the Sear Steak, demonstrating that our results contain more vivid details.

Comparisons on synthetic dataset. In our experiments, we benchmarked 4DGS-1K against several baselines using the monocular synthetic dataset introduced by D-NeRF [19]. The result is shown in Table 2. Compared to 4DGS [1], our method achieves up to $40\times$ compression and $4\times$ faster rendering speed. It is worth noting that the rendering quality of our model even surpasses that of the original 4DGS, with an increase of about $0.38dB$ in PSNR. Furthermore, our approach exhibits higher rendering quality and smaller storage overhead compared to most Gaussian-based methods. We provide qualitative results in Figure 4 for a more visual assessment.

5.3 Ablation Study

To evaluate the contribution of each component, we conducted ablation experiments on the N3V dataset [2]. More ablations are provided in the supplement(See appendix B).

Pruning. As shown in Table 3, our pruning strategy achieves $5\times$ compression ratio and $5\times$ faster rasterization speed while slightly improving rendering quality. As shown in Figure 2a, our pruning strategy also reduces the presence of Gaussians with short lifespan. As such, 4DGS-1k processes far fewer unnecessary Gaussians (See Figure 2b) during rendering. Moreover, as shown in Figure 2c, the pruning process expands the range of adjacent frames. It allows larger intervals for the temporal filter.

Temporal Filtering. As illustrated in Table 3, the results of b and c are obtained by directly applying the filter without fine-tuning. It proves that this component can enhance the rendering speed of 4DGS. However, as mentioned in Section 4.1, the 4DGS contains a huge number of short lifespan Gaussians. It results in some Gaussians being overlooked in the filter, causing a slight decrease in rendering quality. However, through pruning, most Gaussians are ensured to have long lifespan, making them visible even at large intervals. Therefore, it alleviates the issue of Gaussians being overlooked (See f). Furthermore, appropriate fine-tuning allows the Gaussians in the active Gaussians list to relearn the scene features to compensate for the loss incurred by the temporal filter (See e and f).

6 Conclusion

In this paper, we present **4DGS-1K**, a compact and memory-efficient dynamic scene representation capable of running at over 1000 FPS on modern GPUs. We introduce a novel pruning criterion called the spatial-temporal variation score, which eliminates a significant number of redundant Gaussian points in 4DGS, drastically reducing storage requirements. Additionally, we propose a temporal filter that selectively activates only a subset of Gaussians during each frame's rendering. This approach enables our rendering speed to far surpass that of existing baselines. Compared to vanilla 4DGS,

4DGS-1K achieves a $41\times$ reduction in storage and $9\times$ faster rasterization speed while maintaining high-quality reconstruction.

Acknowledgement

This project is supported by the National Research Foundation, Singapore, under its Medium Sized Center for Advanced Robotics Technology Innovation.

References

[1] Zeyu Yang, Hongye Yang, Zijie Pan, and Li Zhang. Real-time photorealistic dynamic scene representation and rendering with 4d gaussian splatting. *arXiv preprint arXiv:2310.10642*, 2023.

[2] Tianye Li, Mira Slavcheva, Michael Zollhoefer, Simon Green, Christoph Lassner, Changil Kim, Tanner Schmidt, Steven Lovegrove, Michael Goesele, Richard Newcombe, et al. Neural 3d video synthesis from multi-view video. In *Proceedings of the IEEE/CVF Conference on Computer Vision and Pattern Recognition*, pages 5521–5531, 2022.

[3] Ben Mildenhall, Pratul P Srinivasan, Matthew Tancik, Jonathan T Barron, Ravi Ramamoorthi, and Ren Ng. Nerf: Representing scenes as neural radiance fields for view synthesis. *Communications of the ACM*, 65 (1):99–106, 2021.

[4] Stephen Lombardi, Tomas Simon, Jason Saragih, Gabriel Schwartz, Andreas Lehrmann, and Yaser Sheikh. Neural volumes: Learning dynamic renderable volumes from images. *arXiv preprint arXiv:1906.07751*, 2019.

[5] Benjamin Attal, Jia-Bin Huang, Christian Richardt, Michael Zollhoefer, Johannes Kopf, Matthew O'Toole, and Changil Kim. Hyperreel: High-fidelity 6-dof video with ray-conditioned sampling. In *Proceedings of the IEEE/CVF Conference on Computer Vision and Pattern Recognition*, pages 16610–16620, 2023.

[6] Sara Fridovich-Keil, Giacomo Meanti, Frederik Rahbæk Warburg, Benjamin Recht, and Angjoo Kanazawa. K-planes: Explicit radiance fields in space, time, and appearance. In *Proceedings of the IEEE/CVF Conference on Computer Vision and Pattern Recognition*, pages 12479–12488, 2023.

[7] Guanjun Wu, Taoran Yi, Jiemin Fang, Lingxi Xie, Xiaopeng Zhang, Wei Wei, Wenyu Liu, Qi Tian, and Xinggang Wang. 4d gaussian splatting for real-time dynamic scene rendering. In *Proceedings of the IEEE/CVF Conference on Computer Vision and Pattern Recognition*, pages 20310–20320, 2024.

[8] Anpei Chen, Zexiang Xu, Andreas Geiger, Jingyi Yu, and Hao Su. Tensorf: Tensorial radiance fields. In *European conference on computer vision*, pages 333–350. Springer, 2022.

[9] Katja Schwarz, Axel Sauer, Michael Niemeyer, Yiyi Liao, and Andreas Geiger. Voxgraf: Fast 3d-aware image synthesis with sparse voxel grids. *Advances in Neural Information Processing Systems*, 35:33999–34011, 2022.

[10] Cheng Sun, Min Sun, and Hwann-Tzong Chen. Direct voxel grid optimization: Super-fast convergence for radiance fields reconstruction. In *Proceedings of the IEEE/CVF conference on computer vision and pattern recognition*, pages 5459–5469, 2022.

[11] Liao Wang, Jiakai Zhang, Xinhang Liu, Fuqiang Zhao, Yanshun Zhang, Yingliang Zhang, Minye Wu, Jingyi Yu, and Lan Xu. Fourier plenoctrees for dynamic radiance field rendering in real-time. In *Proceedings of the IEEE/CVF Conference on Computer Vision and Pattern Recognition*, pages 13524–13534, 2022.

[12] Sara Fridovich-Keil, Alex Yu, Matthew Tancik, Qinhong Chen, Benjamin Recht, and Angjoo Kanazawa. Plenoxels: Radiance fields without neural networks. In *Proceedings of the IEEE/CVF conference on computer vision and pattern recognition*, pages 5501–5510, 2022.

[13] Thomas Müller, Alex Evans, Christoph Schied, and Alexander Keller. Instant neural graphics primitives with a multiresolution hash encoding. *ACM transactions on graphics (TOG)*, 41(4):1–15, 2022.

[14] Christian Reiser, Songyou Peng, Yiyi Liao, and Andreas Geiger. Kilonerf: Speeding up neural radiance fields with thousands of tiny mlps. In *Proceedings of the IEEE/CVF international conference on computer vision*, pages 14335–14345, 2021.

[15] Huan Wang, Jian Ren, Zeng Huang, Kyle Olszewski, Menglei Chai, Yun Fu, and Sergey Tulyakov. R2l: Distilling neural radiance field to neural light field for efficient novel view synthesis. In *European Conference on Computer Vision*, pages 612–629. Springer, 2022.

[16] Bernhard Kerbl, Georgios Kopanas, Thomas Leimkühler, and George Drettakis. 3d gaussian splatting for real-time radiance field rendering. *ACM Trans. Graph.*, 42(4):139–1, 2023.

[17] Ben Mildenhall, Pratul P Srinivasan, Rodrigo Ortiz-Cayon, Nima Khademi Kalantari, Ravi Ramamoorthi, Ren Ng, and Abhishek Kar. Local light field fusion: Practical view synthesis with prescriptive sampling guidelines. *ACM Transactions on Graphics (ToG)*, 38(4):1–14, 2019.

[18] Lingzhi Li, Zhen Shen, Zhongshu Wang, Li Shen, and Ping Tan. Streaming radiance fields for 3d video synthesis. *Advances in Neural Information Processing Systems*, 35:13485–13498, 2022.

[19] Albert Pumarola, Enric Corona, Gerard Pons-Moll, and Francesc Moreno-Noguer. D-nerf: Neural radiance fields for dynamic scenes. In *Proceedings of the IEEE/CVF Conference on Computer Vision and Pattern Recognition*, pages 10318–10327, 2021.

[20] Ang Cao and Justin Johnson. Hexplane: A fast representation for dynamic scenes. In *Proceedings of the IEEE/CVF Conference on Computer Vision and Pattern Recognition*, pages 130–141, 2023.

[21] Liangchen Song, Anpei Chen, Zhong Li, Zhang Chen, Lele Chen, Junsong Yuan, Yi Xu, and Andreas Geiger. Nerfplayer: A streamable dynamic scene representation with decomposed neural radiance fields. *IEEE Transactions on Visualization and Computer Graphics*, 29(5):2732–2742, 2023.

[22] Feng Wang, Sinan Tan, Xinghang Li, Zeyue Tian, Yafei Song, and Huaping Liu. Mixed neural voxels for fast multi-view video synthesis. In *Proceedings of the IEEE/CVF International Conference on Computer Vision*, pages 19706–19716, 2023.

[23] Ziyi Yang, Xinyu Gao, Wen Zhou, Shaohui Jiao, Yuqing Zhang, and Xiaogang Jin. Deformable 3d gaussians for high-fidelity monocular dynamic scene reconstruction. In *Proceedings of the IEEE/CVF Conference on Computer Vision and Pattern Recognition*, pages 20331–20341, 2024.

[24] Zhiyang Guo, Wengang Zhou, Li Li, Min Wang, and Houqiang Li. Motion-aware 3d gaussian splatting for efficient dynamic scene reconstruction. *arXiv preprint arXiv:2403.11447*, 2024.

[25] Zhicheng Lu, Xiang Guo, Le Hui, Tianrui Chen, Min Yang, Xiao Tang, Feng Zhu, and Yuchao Dai. 3d geometry-aware deformable gaussian splatting for dynamic view synthesis. In *Proceedings of the IEEE/CVF Conference on Computer Vision and Pattern Recognition*, pages 8900–8910, 2024.

[26] Jeongmin Bae, Seoha Kim, Youngsik Yun, Hahyun Lee, Gun Bang, and Youngjung Uh. Per-gaussian embedding-based deformation for deformable 3d gaussian splatting. *arXiv preprint arXiv:2404.03613*, 2024.

[27] Devikalyan Das, Christopher Wewer, Raza Yunus, Eddy Ilg, and Jan Eric Lenssen. Neural parametric gaussians for monocular non-rigid object reconstruction. In *Proceedings of the IEEE/CVF Conference on Computer Vision and Pattern Recognition*, pages 10715–10725, 2024.

[28] KL Navaneet, Kossar Pourahmadi Meibodi, Soroush Abbasi Koohpayegani, and Hamed Pirsiavash. Compgs: Smaller and faster gaussian splatting with vector quantization. In *European Conference on Computer Vision*, 2024.

[29] Joo Chan Lee, Daniel Rho, Xiangyu Sun, Jong Hwan Ko, and Eunbyung Park. Compact 3d gaussian representation for radiance field. In *Proceedings of the IEEE/CVF Conference on Computer Vision and Pattern Recognition*, pages 21719–21728, 2024.

[30] Zhiwen Fan, Kevin Wang, Kairun Wen, Zehao Zhu, Dejia Xu, and Zhangyang Wang. Lightgaussian: Unbounded 3d gaussian compression with 15x reduction and 200+ fps. *arXiv preprint arXiv:2311.17245*, 2023.

[31] Guangchi Fang and Bing Wang. Mini-splatting: Representing scenes with a constrained number of gaussians. *arXiv preprint arXiv:2403.14166*, 2024.

[32] Michael Niemeyer, Fabian Manhardt, Marie-Julie Rakotosaona, Michael Oechsle, Daniel Duckworth, Rama Gosula, Keisuke Tateno, John Bates, Dominik Kaeser, and Federico Tombari. Radsplat: Radiance field-informed gaussian splatting for robust real-time rendering with 900+ fps. *arXiv preprint arXiv:2403.13806*, 2024.

[33] Muhammad Salman Ali, Maryam Qamar, Sung-Ho Bae, and Enzo Tartaglione. Trimming the fat: Efficient compression of 3d gaussian splats through pruning. *arXiv preprint arXiv:2406.18214*, 2024.

[34] Panagiotis Papantonakis, Georgios Kopanas, Bernhard Kerbl, Alexandre Lanvin, and George Drettakis. Reducing the memory footprint of 3d gaussian splatting. *Proceedings of the ACM on Computer Graphics and Interactive Techniques*, 7(1):1–17, 2024.

[35] Wenkai Liu, Tao Guan, Bin Zhu, Lili Ju, Zikai Song, Dan Li, Yuesong Wang, and Wei Yang. Efficientgs: Streamlining gaussian splatting for large-scale high-resolution scene representation. *arXiv preprint arXiv:2404.12777*, 2024.

[36] Zhen Xu, Sida Peng, Haotong Lin, Guangzhao He, Jiaming Sun, Yujun Shen, Hujun Bao, and Xiaowei Zhou. 4k4d: Real-time 4d view synthesis at 4k resolution. In *Proceedings of the IEEE/CVF conference on computer vision and pattern recognition*, pages 20029–20040, 2024.

[37] Jonathon Luiten, Georgios Kopanas, Bastian Leibe, and Deva Ramanan. Dynamic 3d gaussians: Tracking by persistent dynamic view synthesis. *arXiv preprint arXiv:2308.09713*, 2023.

[38] Jiahao Wu, Rui Peng, Zhiyan Wang, Lu Xiao, Luyang Tang, Jinbo Yan, Kaiqiang Xiong, and Ronggang Wang. Swift4d: Adaptive divide-and-conquer gaussian splatting for compact and efficient reconstruction of dynamic scene. *arXiv preprint arXiv:2503.12307*, 2025.

[39] Jiawei Xu, Zexin Fan, Jian Yang, and Jin Xie. Grid4d: 4d decomposed hash encoding for high-fidelity dynamic gaussian splatting. *Advances in Neural Information Processing Systems*, 37:123787–123811, 2024.

[40] Zhan Li, Zhang Chen, Zhong Li, and Yi Xu. Spacetime gaussian feature splatting for real-time dynamic view synthesis. In *Proceedings of the IEEE/CVF Conference on Computer Vision and Pattern Recognition*, pages 8508–8520, 2024.

[41] Yuanxing Duan, Fangyin Wei, Qiyu Dai, Yuhang He, Wenzheng Chen, and Baoquan Chen. 4d-rotor gaussian splatting: towards efficient novel view synthesis for dynamic scenes. In *ACM SIGGRAPH 2024 Conference Papers*, pages 1–11, 2024.

[42] Xinjie Zhang, Zhening Liu, Yifan Zhang, Xingtong Ge, Dailan He, Tongda Xu, Yan Wang, Zehong Lin, Shuicheng Yan, and Jun Zhang. Mega: Memory-efficient 4d gaussian splatting for dynamic scenes. *arXiv preprint arXiv:2410.13613*, 2024.

[43] Jiemin Fang, Taoran Yi, Xinggang Wang, Lingxi Xie, Xiaopeng Zhang, Wenyu Liu, Matthias Nießner, and Qi Tian. Fast dynamic radiance fields with time-aware neural voxels. In *SIGGRAPH Asia 2022 Conference Papers*, pages 1–9, 2022.

[44] Yi-Hua Huang, Yang-Tian Sun, Ziyi Yang, Xiaoyang Lyu, Yan-Pei Cao, and Xiaojuan Qi. Sc-gs: Sparse-controlled gaussian splatting for editable dynamic scenes. In *Proceedings of the IEEE/CVF conference on computer vision and pattern recognition*, pages 4220–4230, 2024.

[45] Richard Zhang, Phillip Isola, Alexei A Efros, Eli Shechtman, and Oliver Wang. The unreasonable effectiveness of deep features as a perceptual metric. In *Proceedings of the IEEE conference on computer vision and pattern recognition*, pages 586–595, 2018.

[46] Alex Krizhevsky, Ilya Sutskever, and Geoffrey E Hinton. Imagenet classification with deep convolutional neural networks. *Advances in neural information processing systems*, 25, 2012.

[47] Karen Simonyan and Andrew Zisserman. Very deep convolutional networks for large-scale image recognition. *arXiv preprint arXiv:1409.1556*, 2014.

NeurIPS Paper Checklist

1. **Claims**

   Question: Do the main claims made in the abstract and introduction accurately reflect the paper's contributions and scope?

   Answer: [Yes]

   Justification: The main claims made in the abstract and introduction accurately reflect the paper's contributions and scope.

   Guidelines:

   - The answer NA means that the abstract and introduction do not include the claims made in the paper.
   - The abstract and/or introduction should clearly state the claims made, including the contributions made in the paper and important assumptions and limitations. A No or NA answer to this question will not be perceived well by the reviewers.
   - The claims made should match theoretical and experimental results, and reflect how much the results can be expected to generalize to other settings.
   - It is fine to include aspirational goals as motivation as long as it is clear that these goals are not attained by the paper.

2. **Limitations**

   Question: Does the paper discuss the limitations of the work performed by the authors?

   Answer: [Yes]

   Justification: We discuss it in supplementary material.

   Guidelines:

   - The answer NA means that the paper has no limitation while the answer No means that the paper has limitations, but those are not discussed in the paper.
   - The authors are encouraged to create a separate "Limitations" section in their paper.
   - The paper should point out any strong assumptions and how robust the results are to violations of these assumptions (e.g., independence assumptions, noiseless settings, model well-specification, asymptotic approximations only holding locally). The authors should reflect on how these assumptions might be violated in practice and what the implications would be.
   - The authors should reflect on the scope of the claims made, e.g., if the approach was only tested on a few datasets or with a few runs. In general, empirical results often depend on implicit assumptions, which should be articulated.
   - The authors should reflect on the factors that influence the performance of the approach. For example, a facial recognition algorithm may perform poorly when image resolution is low or images are taken in low lighting. Or a speech-to-text system might not be used reliably to provide closed captions for online lectures because it fails to handle technical jargon.
   - The authors should discuss the computational efficiency of the proposed algorithms and how they scale with dataset size.
   - If applicable, the authors should discuss possible limitations of their approach to address problems of privacy and fairness.
   - While the authors might fear that complete honesty about limitations might be used by reviewers as grounds for rejection, a worse outcome might be that reviewers discover limitations that aren't acknowledged in the paper. The authors should use their best judgment and recognize that individual actions in favor of transparency play an important role in developing norms that preserve the integrity of the community. Reviewers will be specifically instructed to not penalize honesty concerning limitations.

3. **Theory assumptions and proofs**

   Question: For each theoretical result, does the paper provide the full set of assumptions and a complete (and correct) proof?

   Answer: [NA]

Justification: This paper does not involve theoretical result.

Guidelines:

- The answer NA means that the paper does not include theoretical results.
- All the theorems, formulas, and proofs in the paper should be numbered and cross-referenced.
- All assumptions should be clearly stated or referenced in the statement of any theorems.
- The proofs can either appear in the main paper or the supplemental material, but if they appear in the supplemental material, the authors are encouraged to provide a short proof sketch to provide intuition.
- Inversely, any informal proof provided in the core of the paper should be complemented by formal proofs provided in appendix or supplemental material.
- Theorems and Lemmas that the proof relies upon should be properly referenced.

4. **Experimental result reproducibility**

   Question: Does the paper fully disclose all the information needed to reproduce the main experimental results of the paper to the extent that it affects the main claims and/or conclusions of the paper (regardless of whether the code and data are provided or not)?

   Answer: [Yes]

   Justification: The paper discloses all the information needed to reproduce the main experimental results of the paper in Section 5.

   Guidelines:

   - The answer NA means that the paper does not include experiments.
   - If the paper includes experiments, a No answer to this question will not be perceived well by the reviewers: Making the paper reproducible is important, regardless of whether the code and data are provided or not.
   - If the contribution is a dataset and/or model, the authors should describe the steps taken to make their results reproducible or verifiable.
   - Depending on the contribution, reproducibility can be accomplished in various ways. For example, if the contribution is a novel architecture, describing the architecture fully might suffice, or if the contribution is a specific model and empirical evaluation, it may be necessary to either make it possible for others to replicate the model with the same dataset, or provide access to the model. In general. releasing code and data is often one good way to accomplish this, but reproducibility can also be provided via detailed instructions for how to replicate the results, access to a hosted model (e.g., in the case of a large language model), releasing of a model checkpoint, or other means that are appropriate to the research performed.
   - While NeurIPS does not require releasing code, the conference does require all submissions to provide some reasonable avenue for reproducibility, which may depend on the nature of the contribution. For example
     (a) If the contribution is primarily a new algorithm, the paper should make it clear how to reproduce that algorithm.
     (b) If the contribution is primarily a new model architecture, the paper should describe the architecture clearly and fully.
     (c) If the contribution is a new model (e.g., a large language model), then there should either be a way to access this model for reproducing the results or a way to reproduce the model (e.g., with an open-source dataset or instructions for how to construct the dataset).
     (d) We recognize that reproducibility may be tricky in some cases, in which case authors are welcome to describe the particular way they provide for reproducibility. In the case of closed-source models, it may be that access to the model is limited in some way (e.g., to registered users), but it should be possible for other researchers to have some path to reproducing or verifying the results.

5. **Open access to data and code**

   Question: Does the paper provide open access to the data and code, with sufficient instructions to faithfully reproduce the main experimental results, as described in supplemental material?

Answer: [No]

Justification: The code will be open-sourced upon acceptance.

Guidelines:

- The answer NA means that paper does not include experiments requiring code.
- Please see the NeurIPS code and data submission guidelines (`https://nips.cc/public/guides/CodeSubmissionPolicy`) for more details.
- While we encourage the release of code and data, we understand that this might not be possible, so "No" is an acceptable answer. Papers cannot be rejected simply for not including code, unless this is central to the contribution (e.g., for a new open-source benchmark).
- The instructions should contain the exact command and environment needed to run to reproduce the results. See the NeurIPS code and data submission guidelines (`https://nips.cc/public/guides/CodeSubmissionPolicy`) for more details.
- The authors should provide instructions on data access and preparation, including how to access the raw data, preprocessed data, intermediate data, and generated data, etc.
- The authors should provide scripts to reproduce all experimental results for the new proposed method and baselines. If only a subset of experiments are reproducible, they should state which ones are omitted from the script and why.
- At submission time, to preserve anonymity, the authors should release anonymized versions (if applicable).
- Providing as much information as possible in supplemental material (appended to the paper) is recommended, but including URLs to data and code is permitted.

6. **Experimental setting/details**

   Question: Does the paper specify all the training and test details (e.g., data splits, hyperparameters, how they were chosen, type of optimizer, etc.) necessary to understand the results?

   Answer: [Yes]

   Justification: The detailed experiment settings are listed in Section 5.

   Guidelines:

   - The answer NA means that the paper does not include experiments.
   - The experimental setting should be presented in the core of the paper to a level of detail that is necessary to appreciate the results and make sense of them.
   - The full details can be provided either with the code, in appendix, or as supplemental material.

7. **Experiment statistical significance**

   Question: Does the paper report error bars suitably and correctly defined or other appropriate information about the statistical significance of the experiments?

   Answer: [NA]

   Justification: This paper follows the existing work about 4DGS and lists the essential detailed quantitative results in Section 5. None of them report error bars.

   Guidelines:

   - The answer NA means that the paper does not include experiments.
   - The authors should answer "Yes" if the results are accompanied by error bars, confidence intervals, or statistical significance tests, at least for the experiments that support the main claims of the paper.
   - The factors of variability that the error bars are capturing should be clearly stated (for example, train/test split, initialization, random drawing of some parameter, or overall run with given experimental conditions).
   - The method for calculating the error bars should be explained (closed form formula, call to a library function, bootstrap, etc.)
   - The assumptions made should be given (e.g., Normally distributed errors).

- It should be clear whether the error bar is the standard deviation or the standard error of the mean.
- It is OK to report 1-sigma error bars, but one should state it. The authors should preferably report a 2-sigma error bar than state that they have a 96% CI, if the hypothesis of Normality of errors is not verified.
- For asymmetric distributions, the authors should be careful not to show in tables or figures symmetric error bars that would yield results that are out of range (e.g. negative error rates).
- If error bars are reported in tables or plots, The authors should explain in the text how they were calculated and reference the corresponding figures or tables in the text.

8. **Experiments compute resources**

   Question: For each experiment, does the paper provide sufficient information on the computer resources (type of compute workers, memory, time of execution) needed to reproduce the experiments?

   Answer: [Yes]

   Justification: The paper provides sufficient information on the computer resources in Section 5 and supplemental material.

   Guidelines:

   - The answer NA means that the paper does not include experiments.
   - The paper should indicate the type of compute workers CPU or GPU, internal cluster, or cloud provider, including relevant memory and storage.
   - The paper should provide the amount of compute required for each of the individual experimental runs as well as estimate the total compute.
   - The paper should disclose whether the full research project required more compute than the experiments reported in the paper (e.g., preliminary or failed experiments that didn't make it into the paper).

   supplemental material.

9. **Code of ethics**

   Question: Does the research conducted in the paper conform, in every respect, with the NeurIPS Code of Ethics `https://neurips.cc/public/EthicsGuidelines`?

   Answer: [Yes]

   Justification: The research conducted in this paper conform the NeurIPS Code of Ethics.

   Guidelines:

   - The answer NA means that the authors have not reviewed the NeurIPS Code of Ethics.
   - If the authors answer No, they should explain the special circumstances that require a deviation from the Code of Ethics.
   - The authors should make sure to preserve anonymity (e.g., if there is a special consideration due to laws or regulations in their jurisdiction).

10. **Broader impacts**

    Question: Does the paper discuss both potential positive societal impacts and negative societal impacts of the work performed?

    Answer: [Yes]

    Justification: : This paper discusses the potential societal impacts in Section 6 and supplemental material.

    Guidelines:

    - The answer NA means that there is no societal impact of the work performed.
    - If the authors answer NA or No, they should explain why their work has no societal impact or why the paper does not address societal impact.
    - Examples of negative societal impacts include potential malicious or unintended uses (e.g., disinformation, generating fake profiles, surveillance), fairness considerations (e.g., deployment of technologies that could make decisions that unfairly impact specific groups), privacy considerations, and security considerations.

- The conference expects that many papers will be foundational research and not tied to particular applications, let alone deployments. However, if there is a direct path to any negative applications, the authors should point it out. For example, it is legitimate to point out that an improvement in the quality of generative models could be used to generate deepfakes for disinformation. On the other hand, it is not needed to point out that a generic algorithm for optimizing neural networks could enable people to train models that generate Deepfakes faster.
- The authors should consider possible harms that could arise when the technology is being used as intended and functioning correctly, harms that could arise when the technology is being used as intended but gives incorrect results, and harms following from (intentional or unintentional) misuse of the technology.
- If there are negative societal impacts, the authors could also discuss possible mitigation strategies (e.g., gated release of models, providing defenses in addition to attacks, mechanisms for monitoring misuse, mechanisms to monitor how a system learns from feedback over time, improving the efficiency and accessibility of ML).

11. **Safeguards**

    Question: Does the paper describe safeguards that have been put in place for responsible release of data or models that have a high risk for misuse (e.g., pretrained language models, image generators, or scraped datasets)?

    Answer: [NA]

    Justification: This paper does not pose such risk.

    Guidelines:

    - The answer NA means that the paper poses no such risks.
    - Released models that have a high risk for misuse or dual-use should be released with necessary safeguards to allow for controlled use of the model, for example by requiring that users adhere to usage guidelines or restrictions to access the model or implementing safety filters.
    - Datasets that have been scraped from the Internet could pose safety risks. The authors should describe how they avoided releasing unsafe images.
    - We recognize that providing effective safeguards is challenging, and many papers do not require this, but we encourage authors to take this into account and make a best faith effort.

12. **Licenses for existing assets**

    Question: Are the creators or original owners of assets (e.g., code, data, models), used in the paper, properly credited and are the license and terms of use explicitly mentioned and properly respected?

    Answer: [Yes]

    Justification: This paper follows the applicable licenses and terms of usage.

    Guidelines:

    - The answer NA means that the paper does not use existing assets.
    - The authors should cite the original paper that produced the code package or dataset.
    - The authors should state which version of the asset is used and, if possible, include a URL.
    - The name of the license (e.g., CC-BY 4.0) should be included for each asset.
    - For scraped data from a particular source (e.g., website), the copyright and terms of service of that source should be provided.
    - If assets are released, the license, copyright information, and terms of use in the package should be provided. For popular datasets, `paperswithcode.com/datasets` has curated licenses for some datasets. Their licensing guide can help determine the license of a dataset.
    - For existing datasets that are re-packaged, both the original license and the license of the derived asset (if it has changed) should be provided.

- If this information is not available online, the authors are encouraged to reach out to the asset's creators.

13. **New assets**

    Question: Are new assets introduced in the paper well documented and is the documentation provided alongside the assets?

    Answer: [NA]

    Justification: The paper does not release new assets.

    Guidelines:

    - The answer NA means that the paper does not release new assets.
    - Researchers should communicate the details of the dataset/code/model as part of their submissions via structured templates. This includes details about training, license, limitations, etc.
    - The paper should discuss whether and how consent was obtained from people whose asset is used.
    - At submission time, remember to anonymize your assets (if applicable). You can either create an anonymized URL or include an anonymized zip file.

14. **Crowdsourcing and research with human subjects**

    Question: For crowdsourcing experiments and research with human subjects, does the paper include the full text of instructions given to participants and screenshots, if applicable, as well as details about compensation (if any)?

    Answer: [NA]

    Justification: This paper does not involve crowdsourcing nor research with human subjects.

    Guidelines:

    - The answer NA means that the paper does not involve crowdsourcing nor research with human subjects.
    - Including this information in the supplemental material is fine, but if the main contribution of the paper involves human subjects, then as much detail as possible should be included in the main paper.
    - According to the NeurIPS Code of Ethics, workers involved in data collection, curation, or other labor should be paid at least the minimum wage in the country of the data collector.

15. **Institutional review board (IRB) approvals or equivalent for research with human subjects**

    Question: Does the paper describe potential risks incurred by study participants, whether such risks were disclosed to the subjects, and whether Institutional Review Board (IRB) approvals (or an equivalent approval/review based on the requirements of your country or institution) were obtained?

    Answer: [NA]

    Justification: The paper does not involve crowdsourcing nor research with human subjects.

    Guidelines:

    - The answer NA means that the paper does not involve crowdsourcing nor research with human subjects.
    - Depending on the country in which research is conducted, IRB approval (or equivalent) may be required for any human subjects research. If you obtained IRB approval, you should clearly state this in the paper.
    - We recognize that the procedures for this may vary significantly between institutions and locations, and we expect authors to adhere to the NeurIPS Code of Ethics and the guidelines for their institution.
    - For initial submissions, do not include any information that would break anonymity (if applicable), such as the institution conducting the review.

16. **Declaration of LLM usage**

Question: Does the paper describe the usage of LLMs if it is an important, original, or non-standard component of the core methods in this research? Note that if the LLM is used only for writing, editing, or formatting purposes and does not impact the core methodology, scientific rigorousness, or originality of the research, declaration is not required.

Answer: [NA]

Justification: The core method development in this research does not involve LLMs.

Guidelines:

- The answer NA means that the core method development in this research does not involve LLMs as any important, original, or non-standard components.
- Please refer to our LLM policy (`https://neurips.cc/Conferences/2025/LLM`) for what should or should not be described.